



Published in final edited form as:

*Bioorg Med Chem Lett.* 2015 February 1; 25(3): 690–694. doi:10.1016/j.bmcl.2014.11.082.

## Further optimization of the M<sub>5</sub> NAM MLPCN probe ML375: Tactics and challenges

Haruto Kurata<sup>b,c</sup>, Patrick R. Gentry<sup>b,c</sup>, Masaya Kokubo<sup>b,c</sup>, Hyekyung P. Cho<sup>a,b,c</sup>, Thomas M. Bridges<sup>a,b,c</sup>, Colleen M. Niswender<sup>a,b,c</sup>, Frank W. Byers<sup>a,b,c</sup>, Michael R. Wood<sup>a,b,c</sup>, J. Scott Daniels<sup>a,b,c</sup>, P. Jeffrey Conn<sup>a,b,c</sup>, and Craig W. Lindsley<sup>a,b,c,d,\*</sup>

<sup>a</sup>Department of Pharmacology, Vanderbilt University Medical Center, Nashville, TN 37232, USA

<sup>b</sup>Vanderbilt Center for Neuroscience Drug Discovery, Vanderbilt University Medical Center, Nashville, TN 37232, USA

<sup>c</sup>Vanderbilt Specialized Chemistry Center for Probe Development (MLPCN), Nashville, TN 37232, USA

<sup>d</sup>Department of Chemistry, Vanderbilt University, Nashville, TN 37232, USA

### Abstract

This letter describes the continued optimization of the MLPCN probe ML375, a highly selective M<sub>5</sub> negative allosteric modulator (NAM), through a combination of matrix libraries and iterative parallel synthesis. True to certain allosteric ligands, SAR was shallow, and the matrix library approach highlighted the challenges with M<sub>5</sub> NAM SAR within in this chemotype. Once again, enantiospecific activity was noted, and potency at rat and human M<sub>5</sub> were improved over ML375, along with slight enhancement in physiochemical properties, certain *in vitro* DMPK parameters and CNS distribution. Attempts to further enhance pharmacokinetics with deuterium incorporation afforded mixed results, but pretreatment with a *pan*-P450 inhibitor (1-aminobenzotriazole; ABT) provided increased plasma exposure.

### Keywords

M<sub>5</sub>; Muscarinic receptor; Negative allosteric modulator; Matrix library; Pharmacokinetics

Of the five muscarinic acetylcholinereceptors (mAChR subtypes M<sub>1</sub>–M<sub>5</sub>), far less is known about the neurobiological roles of M<sub>5</sub> due both to limited CNS expression (< 2% of all mAChR protein in rat brain and found exclusively in the ventral tegmental area [VTA] on dopamine transporter [DAT]-expressing neurons and in the substantia nigra pars compacta [SNc]) and the lack of highly selective, *in vivo* probe molecules.<sup>1–10</sup> Insight into the therapeutic potential of M<sub>5</sub> comes largely from genetic studies in M<sub>5</sub>-KO mice, which

\*To whom correspondence should be addressed: craig.lindsley@vanderbilt.edu.

**Publisher's Disclaimer:** This is a PDF file of an unedited manuscript that has been accepted for publication. As a service to our customers we are providing this early version of the manuscript. The manuscript will undergo copyediting, typesetting, and review of the resulting proof before it is published in its final citable form. Please note that during the production process errors may be discovered which could affect the content, and all legal disclaimers that apply to the journal pertain.

exhibit reduced sensitivity to the rewarding effects of cocaine and opiates.<sup>11–13</sup> Recently, an association between an M<sub>5</sub> SNP and an addictive phenotype was observed in man, directly linking M<sub>5</sub> to drug abuse and reward.<sup>14</sup> To advance the M<sub>5</sub> research field, small molecule probes are required to recapitulate the genetic data.

Previously, we have reported on the development of several potent and selective M<sub>5</sub> positive allosteric modulator (PAM) chemotypes,<sup>15–18</sup> as well as the first highly M<sub>5</sub> selective orthosteric antagonist;<sup>19</sup> however, DMPK properties were generally poor and these efforts failed to produce *in vivo* probes. Last year we disclosed results from an M<sub>5</sub> functional high-throughput screen that provided 1-(4-fluorobenzoyl)-9b-phenyl-2,3-dihydro-1*H*-imidazo[2,1-*a*]isoindol-5(9*bH*)-one as an M<sub>5</sub> negative allosteric modulator (NAM) hit, **1** (Fig. 1).<sup>20</sup> A limited chemical optimization effort afforded ML375 (**2**), the first M<sub>5</sub>-selective NAM with favorable CNS exposure (brain:plasma  $K_p = 1.8$ ), moderate PK, high plasma protein binding (rat  $f_u = 0.029$ , human  $f_u = 0.013$ , rat brain  $f_u = 0.003$ ) and enantiospecific activity (only the (*S*)-enantiomer of the 9b *p*-Cl phenyl was active).<sup>20</sup> Despite a major advance in the field, due to weak potency at rat M<sub>5</sub>, coupled with high plasma protein and brain homogenate binding, ML375 lacked the requisite free drug exposure to serve as an *in vivo* tool compound.<sup>20</sup> In this Letter, we report on the continued optimization of our first-in-class M<sub>5</sub> NAM, and detail key tactics and noteworthy challenges en route to an M<sub>5</sub> NAM *in vivo* probe.

The synthesis of novel analogs of ML375 required a simple two-step synthesis involving condensation of ethylene diamine and an appropriately substituted 2-benzoylbenzoic acid **3** (or heteroaromatic/cyclo(hetero)alkyl congener) to provide **4**, followed by a subsequent acylation reaction (Scheme 1) to deliver ML375 analogs **5–7**.<sup>20,21</sup> However, we quickly exhausted the commercial analogs of **3**. Fortunately, we were able to employ three synthetic routes to access key intermediates **3** with either diverse substituents or encompassing heterocycles.

In the first round of library synthesis, we held the *p*-Cl 9b phenyl moiety of ML375 constant, and scanned alternate amides within a racemic core to provide analogs **5**. Here, (Table 1) we found that heterocycles were generally not tolerated (**5i-l**) in the context of the *p*-Cl 9b phenyl core, but two amide congeners, the 4-isopropoxyphenyl (**5f**) and the 3,4,5-trifluorophenyl (**5g**), displayed submicromolar human M<sub>5</sub> activity (hM<sub>5</sub> IC<sub>50</sub>s of 790 nM and 610 nM, respectively), yet were less potent than racemic ML375 (**5a**, hM<sub>5</sub> IC<sub>50</sub> = 480 nM). Within a conserved series of ethers, hM<sub>5</sub> potency, e.g. M<sub>5</sub> IC<sub>50</sub>s, was enhanced as steric bulk increased<sup>22</sup> - OMe (**5d**) < OEt (**5e**) < *Oi*-Pr (**5f**). Despite the lower hM<sub>5</sub> potency, **5d** displayed a moderate improvement in clogP relative to **5a** (4.6 versus 5.2), so we elected to evaluate how diminished lipophilicity would impact plasma protein binding. While racemic **5a** displayed high plasma protein binding (rat  $f_u = 0.031$ , human  $f_u = 0.015$ ), binding of **5f** was slightly decreased (rat  $f_u = 0.037$ , human  $f_u = 0.027$ ). These findings then led us to pursue second generation libraries where we aimed to incorporate polar, basic and sp<sup>3</sup>-hybridized ring systems into the 9b position, while holding the 3,4-difluorobenzoyl moiety constant, to assess if we could improve both physicochemical properties as well as hM<sub>5</sub> potency.

Following scheme 1, analogs **6** were rapidly prepared and screened against hM<sub>5</sub> (Table 2). Once again, SAR was shallow, with all sp<sup>3</sup>-based systems, as well as heterocycles, devoid of hM<sub>5</sub> activity. A similar pattern emerged for ethers between analog series **5** and **6**, with **6c**, the 4-OMe phenyl analog, superior potency (hM<sub>5</sub> IC<sub>50</sub> = 1.3 μM), but insufficient to advance as an *in vivo* probe. As before, **6c** possessed a lower clogP (4.21), which translated into improved plasma free fraction (rat  $f_u$  = 0.064, human  $f_u$  = 0.037). Interestingly, the addition of more sp<sup>3</sup>-character, in the form of the cyclohexyl congener **6e**, led to a higher clogP (5.2) and diminished free fraction (rat  $f_u$  = 0.016, human  $f_u$  = 0.008). In parallel, we replaced the phenyl ring at the 9b position with the three regioisomeric pyridines, and all were not tolerated (hM<sub>5</sub> IC<sub>50</sub> > 5 μM), as were ring expansions and substitutions of the 1*H*-imidazo[2,1-*a*]isoindol-5(9*bH*)-one core.

At a loss for a rational, singleton approach to build-in hM<sub>5</sub> potency and improved physiochemical properties, we elected to pursue a 3 × 9 matrix library of analogs **7** to systematically evaluate all the possible combinations of monomers that showed either hM<sub>5</sub> potency enhancement or improved physiochemical properties (Table 3).<sup>22,23</sup> While we have generated, on numerous occasions, robust, tractable SAR within GPCR allosteric ligand chemotypes, we have also reported on numerous accounts of chemotypes that possess shallow or flat SAR,<sup>8–11,24</sup> and this matrix library is an example of the latter. Here, the clear stand-out was racemic **7B-6** (also referred to as VU0652483, hM<sub>5</sub> IC<sub>50</sub> = 517 nM, pIC<sub>50</sub> = 6.29±0.02), possessing a 3,4,5-trifluorobenzoyl amide and a 3-methyl-4-methoxy phenyl moiety in the 9b position. Due to the increased hM<sub>5</sub> potency, we evaluated VU0652483 potency at rat M<sub>5</sub> and found submicromolar activity (rat M<sub>5</sub> IC<sub>50</sub> = 963 nM, pIC<sub>50</sub> = 6.02±0.04) as well. As all of the activity of ML375 resided in the (*S*)-enantiomer, we resolved the enantiomers of VU0652483 via chiral SFC to afford (*S*)-**7B-6** (VU6000181) and (*R*)-**7B-6** (VU6000180); here again, the (*R*)-enantiomer was inactive (Fig. 2) and the (*S*)-enantiomer, VU6000181, possessed all of the M<sub>5</sub> M<sub>5</sub> NAM reported to date and maintaining selectivity versus M<sub>1</sub>–M<sub>4</sub> (IC<sub>50s</sub> > 30 μM).<sup>20</sup> Moreover, the clogP for VU6000181 (4.6) was improved over ML375 (5.2), and this once again translated into a slight improvement over ML375 (rat  $f_u$  = 0.031, human  $f_u$  = 0.013, rat brain  $f_u$  = 0.006). In addition, VU6000181 was highly centrally penetrant (brain:plasma  $K_p$  = 2.7 at 0.25 ht post-administration), yet a high clearance compound *in vitro* (rat hepatic microsome CL<sub>INT</sub> = 332 mL/min/kg, predicted CL<sub>HEP</sub> = 57.8 mL/min/kg and human hepatic microsome CL<sub>INT</sub> = 359 mL/min/kg, predicted CL<sub>HEP</sub> = 19.8 mL/min/kg) and *in vivo* (rat CL<sub>p</sub> = 80 mL/min/kg, t<sub>1/2</sub> = 65 min, V<sub>ss</sub> = 4.9 L/kg). The PK profile of VU6000181 rendered it unsuitable as an *in vivo* probe.

Previously, we productively utilized deuterium incorporation to overcome high clearance coupled with flat SAR in a series of mGlu<sub>3</sub> NAMs,<sup>25</sup> reducing rat *in vitro* and *in vivo* clearance by ~50% and affording an *in vivo* probe. Replacing the OCH<sub>3</sub> moiety of VU6000181 with a OCD<sub>3</sub> moiety (**10**, VU6001005) did in fact reduce human *in vitro* intrinsic clearance ~5-fold (human CL = 72.9 mL/min/kg) but provided negligible improvement to rat intrinsic clearance, and thus, was not a productive path towards an *in vivo* tool compound (Fig. 3).

Finally, we performed an *in vivo* PK study by pre-dosing rats with the *pan*-P450 inhibitor 1-aminobenzotriazole (ABT) in an attempt to potentially achieve therapeutically relevant drug levels and provide target validation for M<sub>5</sub> NAMs.<sup>26</sup> In this instance, we first pre-treated rats with an oral vehicle (10% tween 80 in 0.5% MC in water), followed 1.5 hours later by VU6000181 at 10 mg/kg, P.O. in 30% HPBCD in water (10 mg/mL). This control protocol revealed a VU6000181 mean residence time (MRT) of 6.5 hours, a T<sub>max</sub> of 2.8 hours, an AUC<sub>0-inf</sub> of 3,600 (hr\*ng/mL) and low oral bioavailability (%F = 2.0). Pre-treatment of rats with a 56.6 mg/kg dose of ABT P.O. (10% tween 80 in 0.5% MC in water), followed 1.5 hours later by VU6000181 at 10 mg/kg, P.O. in 30% HPBCD in water (10 mg/mL), provided a ~5-fold increase in exposure (AUC<sub>0-inf</sub> 17,700 (hr\*ng/mL), %F = 9.5) relative to that in the vehicle pre-treated animals (Fig. 4). In addition, ABT pre-treatment afforded a ~3-fold increase in C<sub>max</sub> (plasma = 2.0 μM, ~ 62 nM unbound) and, based on the a brain:plasma K<sub>p</sub> (2.7), projected C<sub>max</sub> levels in brain in the presence of ABT would be ~ 5.4 μM (~ 32 nM unbound). Thus, ABT pretreatment may serve as a viable strategy to increase levels of VU6000181 for future fMRI and addiction studies to test selective M<sub>5</sub> inhibition hypotheses.

In summary, we reported on the continued optimization of the MLPCN probe ML375, a highly selective M<sub>5</sub> NAM, through a combination of matrix libraries and iterative parallel synthesis. While SAR can be highly tractable for certain allosteric ligands, this chemotype was a clear example of 'flat' or 'shallow' SAR, wherein a matrix library was critical in identifying a productive lead compound, VU6000181, with improved activity at rat M<sub>5</sub> and disposition relative to ML375. Attempts to improve PK by deuterium incorporation substantially impacted only human *in vitro* CL<sub>INT</sub>, but ABT pre-treatment significantly increased exposure in rats, potentially affording a strategy to achieve target validation for selective M<sub>5</sub> inhibition. Efforts continue, and work is in progress to pharmacologically probe M<sub>5</sub> neurobiology and therapeutic potential with small molecules.

## Acknowledgments

Vanderbilt is a member of the MLPCN and houses the Vanderbilt Specialized Chemistry Center for Accelerated Probe Development. This work was supported by the NIH/MLPCN grant U54 MH084659 (C.W.L.), the Vanderbilt Department of Pharmacology and William K. Warren, Jr. who funded the William K. Warren, Jr. Chair in Medicine (to C.W.L.).

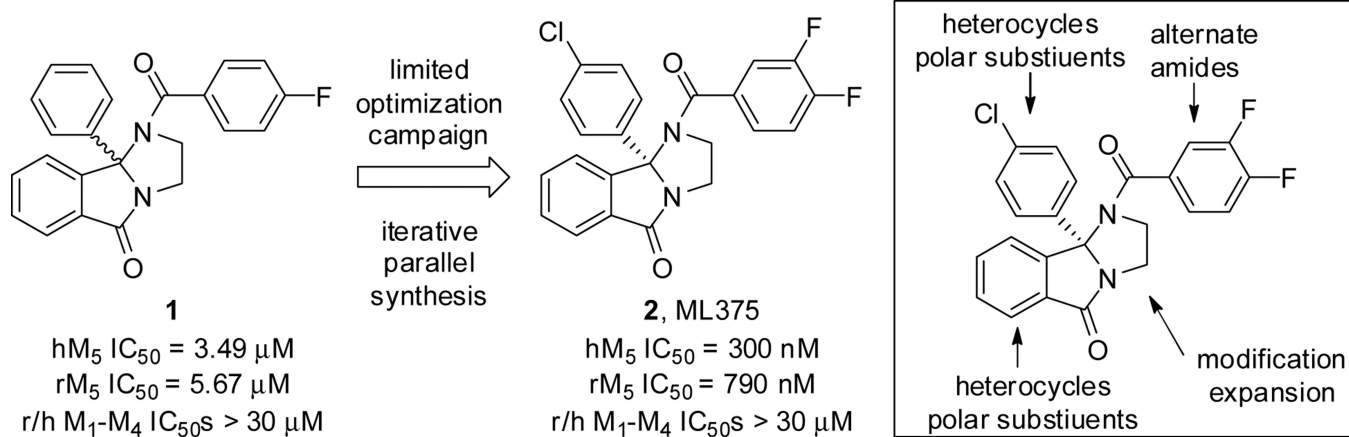
## References

1. Smythies J. *Int. Rev. Neurobiol.* 2005; 64:1–122. [PubMed: 16096020]
2. Wess J, Eglén RM, Gautam D. *Nat. Rev. Drug Discov.* 2007; 6:721–733. [PubMed: 17762886]
3. Langmead CJ, Watson J, Reavill C. *Pharmacol. Ther.* 2008; 117:232–243. [PubMed: 18082893]
4. Denker D, Thomsen M, Wortwein G, Weikop G, Cui Y, Jeon J, Wess J, Fink-Jensen A. *ACS Chem. Neurosci.* 2012; 3:80–89. [PubMed: 22389751]
5. Caulfield MP, Birdsall NJM. *Pharmacol. Rev.* 1998; 50:279–290. [PubMed: 9647869]
6. Weiner DM, Levey AI, Brann MR. *Proc. Natl. Acad. Sci. U.S.A.* 1990; 87:7050–7054. [PubMed: 2402490]
7. Yasuda RP, Ciesla W, Flores LR, Wall SJ, Li M, Satkus SA, Weisstein JS, Spagnola BV, Wolfe BB. *Mol. Pharmacol.* 1993; 43:149–157. [PubMed: 8429821]
8. Melancon BJ, Hopkins CR, Wood MR, Emmitte KA, Niswender CM, Christopoulos A, Conn PJ, Lindsley CW. *J. Med. Chem.* 2012; 55:1445–1464. [PubMed: 22148748]

9. Conn PJ, Jones C, Lindsley CW. Trends in Pharm. Sci. 2009; 30:148–156. [PubMed: 19201489]
10. Lindsley CW. J. Med. Chem. 2014; 57:7485–7498. [PubMed: 25180768]
11. Basile AS, Fedorova I, Zapata A, Liu X, Shippenberg T, Yamada M, Wess J. Proc. Natl. Acad. Sci. U.S.A. 2002; 99:11452–11457. [PubMed: 12154229]
12. Fink-Jensen A, Fedorova I, Wörtwein G, Woldbye DP, Thomsen M, Bolwig TG, Knitowski KM, McKinzie DL, Yamada M, Wess J, Basile AJ. Neurosci. Res. 2003; 74:91–96.
13. Thomsen M, Woldbye DP, Wortwein G, Fink-Jensen A, Wess J, Caine SB. Neurosci. 2005; 25:8141–8149.
14. Anney RJJ, Lotfi-Miri M, Olsson CA, Reid SC, Hemphill SA, Patton GC. BMC Genet. 2007; 8:46. [PubMed: 17608938]
15. Bridges TM, Marlo JE, Niswender CM, Jones JK, Jadhav SB, Gentry PR, Weaver CD, Conn PJ, Lindsley CW. J. Med. Chem. 2009; 52:3445–3448. [PubMed: 19438238]
16. Bridges TM, Kennedy JP, Hopkins CR, Conn PJ, Lindsley CW. Bioorg. Med. Chem. Lett. 2010; 20:5617–5622. [PubMed: 20801651]
17. Gentry PR, Bridges TM, Lamsal A, Vinson PN, Smith E, Chase P, Hodder PS, Engers JL, Niswender CM, Daniels JS, Conn PJ, Wood MR, Lindsley CW. Bioorg. Med. Chem. Lett. 2013; 23:2996–3000. [PubMed: 23562060]
18. Gentry PR, Kokubo M, Bridges TM, Byun N, Cho HP, Smith E, Hodder PS, Niswender CM, Daniels JS, Conn PJ, Lindsley CW, Wood MR. J. Med. Chem. 2014; 57:7804–7810. [PubMed: 25147929]
19. Gentry PR, Kokubo M, Bridges TM, Cho HP, Smith E, Chase P, Hodder PS, Utley TJ, Rajapakse A, Byers F, Niswender CM, Morrison RD, Daniels JS, Wood MR, Conn PJ, Lindsley CW. Chem Med Chem. 2014; 9:1677–1682. [PubMed: 24692176]
20. Gentry PR, Kokubo M, Bridges TM, Kett NR, Harp JM, Cho HP, Smith E, Chase P, Hodder PS, Niswender CM, Daniels SJ, Conn PJ, Wood MR, Lindsley CW. J. Med. Chem. 2013; 56:9351–9355. [PubMed: 24164599]
21. Synthesis of VU6000181. To a suspension of Mg (936 mg, 38.5 mmol) and iodine (5 mg) in THF (2 mL) was added a part of a solution of 4-bromo-2-methylanisole (7.39 g, 36.8 mmol) in THF (9 mL) at ambient temperature. After initiating the reaction, a solution of 4-bromo-2-methylanisole diluted with THF (19 mL) was added dropwise to the mixture diluted with THF (10 mL). After the mixture was allowed to stir at ambient temperature for 2 hours, resulting Grignard reagent was added to a suspension of phthalic anhydride **8** (5.18 g, 35.0 mmol) in THF (50 mL) at –65 °C. The mixture was allowed to stir for 2.5 hours as temperature was elevated up to 0 °C. The reaction was quenched with cold water and the aqueous layer was separated. The organic layer was extracted with 1 N NaOH aqueous solution and the combined aqueous layer was acidified with 2 N HCl solution. The aqueous layer was extracted with ethyl acetate twice and the combined organic layer was washed with brine and dried over magnesium sulfate. The filtrate was evaporated under reduced pressure. The residue was triturated with ethyl acetate/diethyl ether to give compound **3** as a white powder (5.61 g, 59% yield). To a solution of compound **3** (1.0 g, 3.7 mmol) and *para*-toluenesulfonic acid monohydrate (10 mg) in PhMe (8 mL) and 1,4-dioxane (8 mL) was added ethylenediamine (0.50 mL, 7.4 mmol) at ambient temperature. The resulting white suspension was subjected to microwave irradiation at 150 °C for 30 minutes. After removing insoluble material, the filtrate was concentrated. The procedure above was repeated twice more and the three portions were combined and purified on silica gel using hexane/ethyl acetate as an eluent. Crude product was triturated with diethyl ether to give compound **4** as an off-white powder (1.69 g, 52% yield). To a solution of compound **4** (500 mg, 1.70 mmol) in dichloromethane (8 mL) was added DIPEA (0.74 mL, 4.25 mmol) and 3,4,5-trifluorobenzoyl chloride (0.33 mL, 2.55 mmol) at ambient temperature. After stirring for 30 minutes, cold NaHCO<sub>3</sub>-aq was added to the mixture which was extracted with dichloromethane twice. The combined organic layer was concentrated under reduced pressure and the residue was purified on silica gel using hexane/ethyl acetate as an eluent. Crude product was triturated with diethyl ether/hexane to yield compound **7B-6** as a white powder (491 mg, 64% yield). Chiral resolution by SFC (Agilent 1260, Column: LUX cellulose-3, Column dimensions: 10 × 250 mm, Co-solvent: MeOH, Modifier: none, Gradient Profile: 10% isocratic, Flow Rate: 15 mL/min, Backpressure: 100, Column temperature: 40 degrees, retention time: 2.814 min, 30 dated on July 30<sup>th</sup>) followed by concentration afforded (*S*)-**7B-6** (**VU6000181**) as a white

powder.  $^1\text{H}$  NMR (400.1 MHz, DMSO-*d*<sub>6</sub>): 7.89 (d, *J* = 7.4 Hz, 1H), 7.80-7.71 7.78 (m, 1H), 7.71-7.57 (m, 4H), 7.03 (dd, *J* = 8.5, 2.5 Hz, 1H), 6.91 (d, *J* = 8.5 Hz, 1H), 6.86 (d, *J* = 2.5 Hz, 1H), (dt, *J* = 252, 15.6 Hz), 133.87, 133.68 (q, *J* = 6.1 Hz), 132.84, 131.18, 130.35, 129.48, 128.74, 126.61, 125.75, 124.18, 113.29 (dd, *J* = 16.5, 6.0 Hz), 110.94, 87.66, 56.25, 52.45, 40.24, 17.11. HRMS calc'd for: C<sub>25</sub>H<sub>19</sub>F<sub>3</sub>N<sub>2</sub>O<sub>3</sub> (M+H), 425.1348; found 452.1352. Specific rotation  $[\alpha]_D^{23} = -169^\circ$  (*c* = 0.75, CHCl<sub>3</sub>).

22. Lavieri R, Scott SA, Selvy PE, Brown HA, Lindsley CW. *J. Med. Chem.* 2010; 53:6706–6719. [PubMed: 20735042]
23. Kennedy JP, Williams L, Bridges TM, Daniels RN, Weaver D, Lindsley CW. *J. Comb. Chem.* 2008; 10:345–354. [PubMed: 18220367]
24. Zhao Z, Wisnoski DD, O'Brien JA, Lemiare W, Williams DL Jr, Jacobson MA, Wittman M, Ha S, Schaffhauser H, Sur C, Pettibone DJ, Duggan ME, Conn PJ, Hartman GD, Lindsley CW. *Bioorg. Med. Chem. Lett.* 2007; 17:1386–1389. [PubMed: 17210250]
25. Wenthur CJ, Niswender CM, Morrison R, Daniels JS, Conn PJ, Lindsley J. *J. Med. Chem.* 2013; 56:5208–5212. [PubMed: 23718281]
26. Mico BA, Federowicz DA, Ripple MG, Kerns W. *Biochem. Pharmacol.* 1988; 37:2515–2519. [PubMed: 3390214]

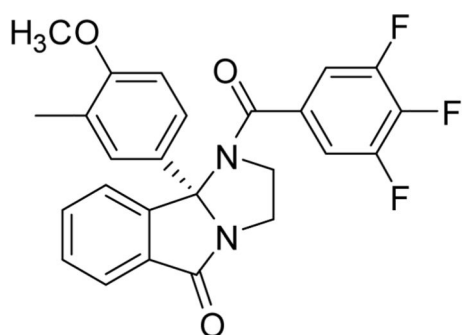
**Figure 1.**

Structures and mAChR activities of  $M_5$  NAM HTS hit **1**, and the optimized MLPCN probe ML375 (**2**). Inset, optimization plan for ML375 to improve rat potency and physiochemical/disposition properties. Potency values determined via a functional calcium mobilization assay in the presence of a fixed acetylcholine  $EC_{80}$  in recombinant cells.<sup>20</sup>



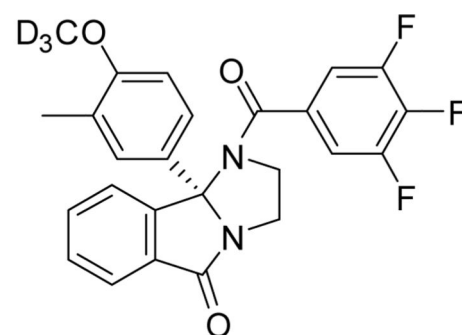
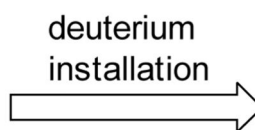




**7B-6**, VU6000181

human  $CL_{INT}$  = 359 mL/min/kg  
 human  $CL_{HEP}$  = 19.8 mL/min/kg

rat  $CL_{INT}$  = 332 mL/min/kg  
 rat  $CL_{HEP}$  = 57.8 mL/min/kg

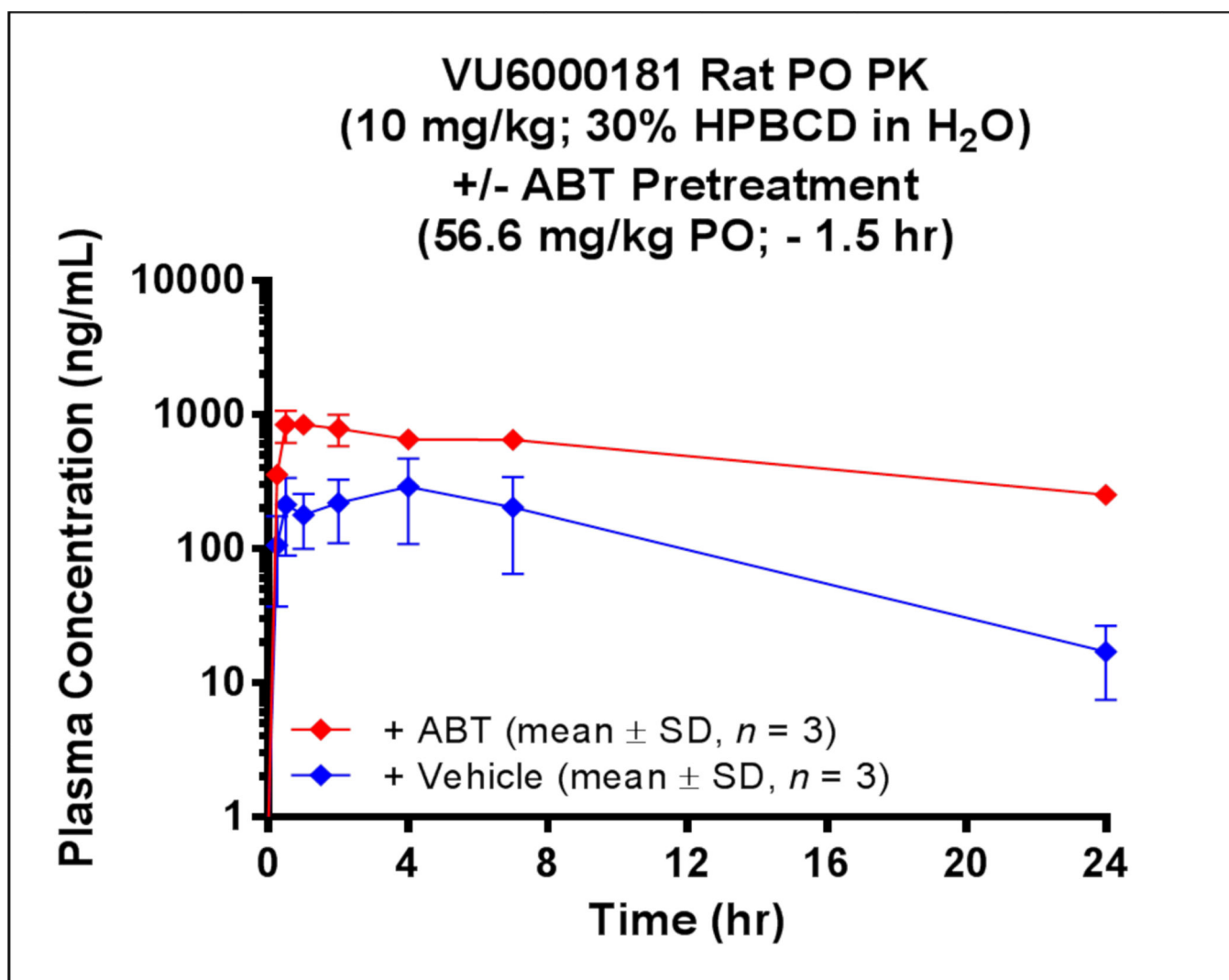
**10**, VU6001005

human  $CL_{INT}$  = 72.9 mL/min/kg  
 human  $CL_{HEP}$  = 16.3  
 mL/min/kg

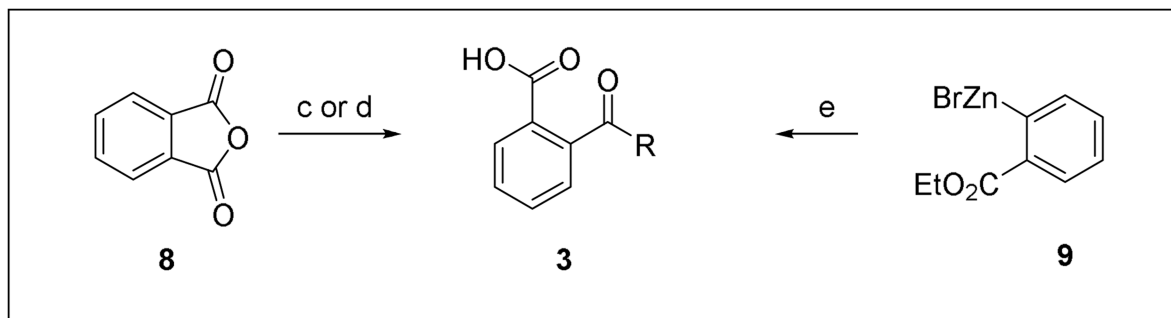
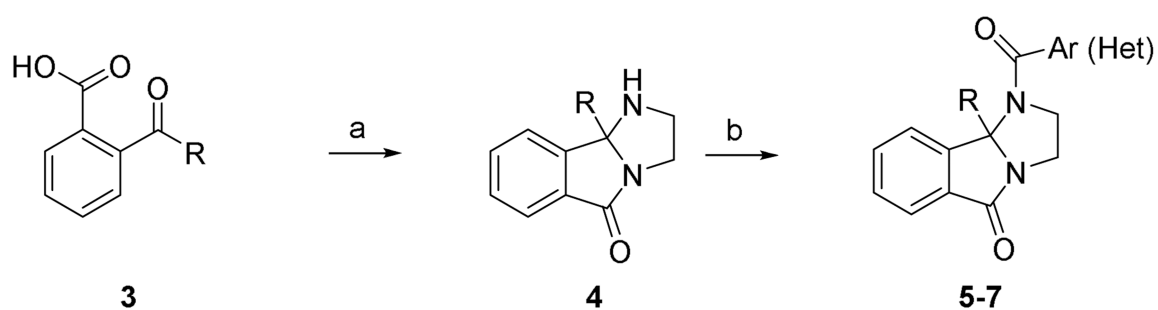
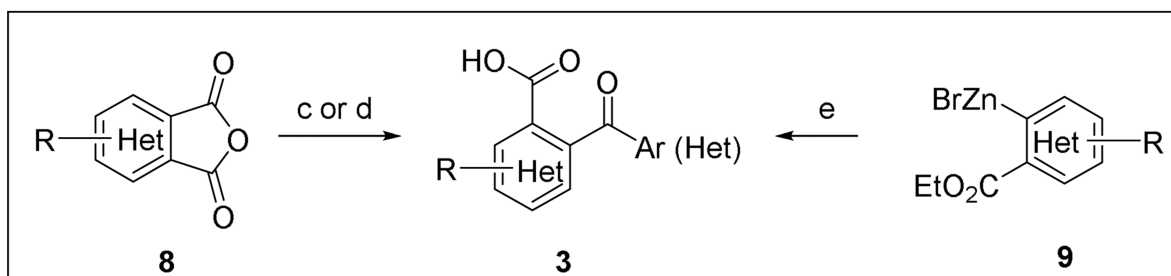
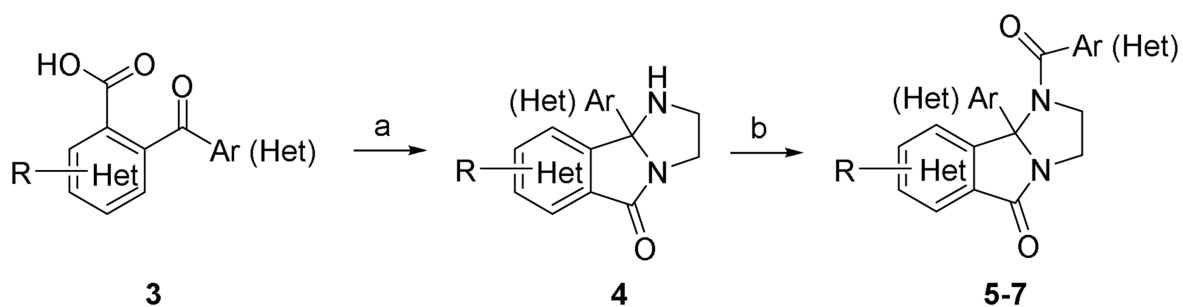
rat  $CL_{INT}$  = 275 mL/min/kg  
 rat  $CL_{HEP}$  = 55.8 mL/min/kg

**Figure 3.**

The impact of deuterium incorporation into VU6000181 on human, but not rat, intrinsic clearance determined in hepatic microsomes fortified with NADPH (values represent means from one independent determination performed in triplicate).

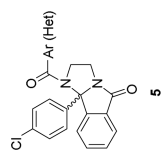


**Figure 4.** Oral plasma pharmacokinetics of VU6000181 in the absence (blue) or presence (red) of ABT pre-treatment in rats (male, Sprague-Dawley). ABT pre-treatment improved exposure ~ 5-fold and maximum concentrations ~ 3-fold.

**Scheme 1.**

Reagents and conditions: (a) ethylene diamine, *p*-TSA, toluene (+1,4-dioxane), reflux, Dean-Stark trap, or microwave irradiation 130–150 °C 4–77%; (b) Ar(Het)COCl, CH<sub>2</sub>Cl<sub>2</sub>, DIPEA, 16–91%; (c) RMgX, THF, –65 °C to 0 °C or rt, 8–68%; (d) R-H, AlCl<sub>3</sub>, PhNO<sub>2</sub>, rt, 41–88%; (e) *i.* RCOCl, cat. Ni(acac)<sub>2</sub>, THF, rt, *ii.* Aq. NaOH, EtOH/THF, rt, 31–55%.

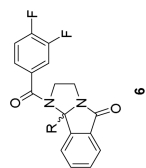
Table 1

Structures and activities of analogs **5**.

Entry	Ar(Het)	hM <sub>5</sub> IC <sub>50</sub> (μM)	hM <sub>5</sub> pIC <sub>50</sub> <sup>a</sup>	Entry	Ar(Het)	hM <sub>5</sub> IC <sub>50</sub> (μM)	hM <sub>5</sub> pIC <sub>50</sub> <sup>a</sup>
<b>5a</b>		0.48	6.32±0.03	<b>5g</b>		0.61	6.21±0.02
<b>5b</b>		>10	>5	<b>5h</b>		>10	>5
<b>5c</b>		6.6	5.18±0.16	<b>5i</b>		>10	>5
<b>5d</b>		1.8	5.74±0.08	<b>5j</b>		5.8	5.23±0.09
<b>5e</b>		0.85	6.07±0.05	<b>5k</b>		>10	>5
<b>5f</b>		0.79	6.10±0.03	<b>5l</b>		>10	>5

<sup>a</sup> hM<sub>5</sub> pIC<sub>50</sub> reported as average ±SEM from our calcium mobilization assay; n = 3.

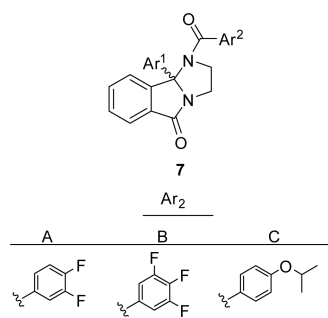
Table 2

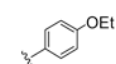
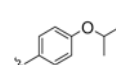
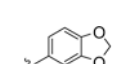
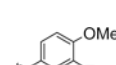
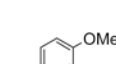
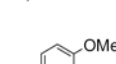
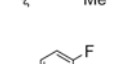
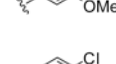
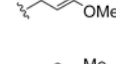
Structures and activities of analogs **6**.

Entry	R	hM <sub>5</sub> IC <sub>50</sub> (μM)	hM <sub>5</sub> pIC <sub>50</sub> <sup>a</sup>	Entry	R	hM <sub>5</sub> IC <sub>50</sub> (μM)	hM <sub>5</sub> pIC <sub>50</sub> <sup>a</sup>
<b>6a</b>		5.5	5.25±0.07	<b>6g</b>		>10	>5
<b>6b</b>		1.6	5.79±0.04	<b>6h</b>		>10	>5
<b>6c</b>		1.3	5.88±0.01	<b>6i</b>		>10	>5
<b>6d</b>		>10	>5	<b>6j</b>		>10	>5
<b>6e</b>		2.1	5.67±0.05	<b>6k</b>		>10	>5
<b>6f</b>		2.4	5.61±0.06	<b>6l</b>		>10	>5

<sup>a</sup>hM<sub>5</sub> pIC<sub>50</sub> reported as average ±SEM from our calcium mobilization assay; n = 3.

Table 3

Structures and activities of matrix library analogs **7**.


Entry	hM <sub>5</sub> IC <sub>50</sub> (μM) <sup>a</sup>	hM <sub>5</sub> IC <sub>50</sub> (μM) <sup>a</sup>	hM <sub>5</sub> IC <sub>50</sub> (μM) <sup>a</sup>	
1	3.2	>30	4.1	
2	>30	2.4	1.9	
3	1.3	1.0	1.1	
4	3.3	>30	3.2	
5	5.5	1.4	3.3	
6	1.2	0.51	1.3	
7	2.7	0.7	1.3	
8	2.0	1.6	6.4	
9	1.3	0.9	2.2	

<sup>a</sup>hM<sub>5</sub> IC<sub>50</sub> data, n = 1; hM<sub>5</sub> IC<sub>50</sub> for **7B-6**, n = 6, pIC<sub>50</sub> = 6.29±0.02